Improving Prostamide Anti-Cancer Activity Through Derivatization and Micellar Delivery

By

David Halatek

May, 2023

Director of Thesis: Dr. Colin Burns

Major Department: Chemistry

ABSTRACT

Colorectal cancer is the fourth most common cancer diagnosis per year as well as the fourth highest rate of death per year according to the Centers for Disease Control. Approximately 1/3rd of the diagnosed colorectal cancer cases per year will result in death.[1] Prior research from our group has shown that the prostaglandin-ethanolamide 15-deoxy, $\Delta^{12,14}$ prostamide J_2 (15d-$\Delta^{12,14}$-PMJ_2) is selectively toxic to murine melanoma cells (B16F10) and murine colorectal cells (CT-26) both *in vitro* and *in vivo* and significantly reduces tumor growth.[2] Further, 15d-$\Delta^{12,14}$-PMJ_2 induces cell death in primary patient melanoma cells and thus may be a promising therapeutic. As 15d-$\Delta^{12,14}$-PMJ_2 can be made by the condensation of ethanolamine with 15-deoxy, $\Delta^{12,14}$ prostaglandin J_2 (15d-$\Delta^{12,14}$-PGJ_2), we sought to test the cytotoxicity of other prostamide derivatives to determine the structural features required for activity. Based on prior results in a study of related prodrugs, 15d-$\Delta^{12,14}$-PMJ_2-Arvanil was selected as the top candidate for testing anti-cancer activity. After testing in both a human and murine cell line, it was determined that 15d-$\Delta^{12,14}$-PMJ_2-Arvanil was not as cytotoxic as 15d-$\Delta^{12,14}$-PMJ_2. It is possible that the bulkier functional group on the α-chain of the prostamide prevents transport into the cell the same way or to the same degree 15d-$\Delta^{12,14}$-PMJ_2 enters. In an effort to test this hypothesis,

and to develop an improved means for systemic delivery for this class of hydrophobic prostamides, engineered micelles composed of 1,2-distearoyl-sn-glycero-3-phosphoethanolamine-N-[methoxy(polyethylene glycol)-2000] and D-α-tocopherol polyethylene glycol 1000 succinate were investigated as drug carriers

Improving Prostamide Anti-Cancer Activity Through Derivatization and Micellar Delivery

A Thesis

Presented to the Faculty of the Department Chemistry

East Carolina University

In Partial Fulfillment of the Requirements for the Degree

Master of Science in Chemistry

By

David Halatek

May, 2023

Director of Thesis: Colin Burns, PhD
Thesis Committee Members:
William Allen, PhD
Robert Hughes, PhD
Rukiyah Van Dross, PhD

Table of Contents

Table of Figures

LIST OF ABBREVIATIONS

Chapter One: Introduction

1.1: Cancer

Cancer is responsible for a quarter of deaths in the United States. Cancer is defined as uncontrolled cell growth, oftentimes without the presence of cell growth signals, and invasion into other tissues in the body.[3] This uncontrolled cell growth usually results from mutations in cell signaling and apoptosis pathways. These mutations can be accumulated through environmental damage, such as exposure to ultraviolet light or carcinogenic chemicals, natural errors as a result of cell division or inherited errors usually present since birth. The damage/mutations will often accumulate in three main types of genes: DNA repair genes, proto-oncogenes, and tumor suppression genes. These are genes that are responsible for controlling cell growth, correcting DNA damage, or beginning the apoptosis pathway if there is too much damage. Once surviving the initial growth period to successfully become a tumor, additional changes will begin that designate this growth as cancer. The first is angiogenesis, which is the process of encouraging very rapid growth of blood vessels to the tumor to provide nutrients to the rapidly growing tumor. These cells also tend to develop mutations that bypass the immune system. Some develop the ability to use different nutrients compared to normal cells.[3]

1.1.1: Colorectal Cancer

Colorectal cancer is the fourth most common cancer diagnosis per year as well as the fourth highest rate of death per year according to the Centers for Disease Control. Approximately 1/3rd of the diagnosed colorectal cancer cases per year will result in death.[1] Colorectal cancer, also known as colon or rectal cancer, most often begins as polyps in the mucosa of the colon or rectum as seen in Figure 1. Not all polyps result in cancer but, of the three types, two have a

much higher chance of developing into cancer over time. As a result of this, most colorectal cancers are adenocarcinomas meaning they began as cells that produce mucus to lubricate the inside of the colon and rectum. As the cancer grows in the wall of the intestines it begins to gain access to blood and lymph vessels that may result in metastasis.

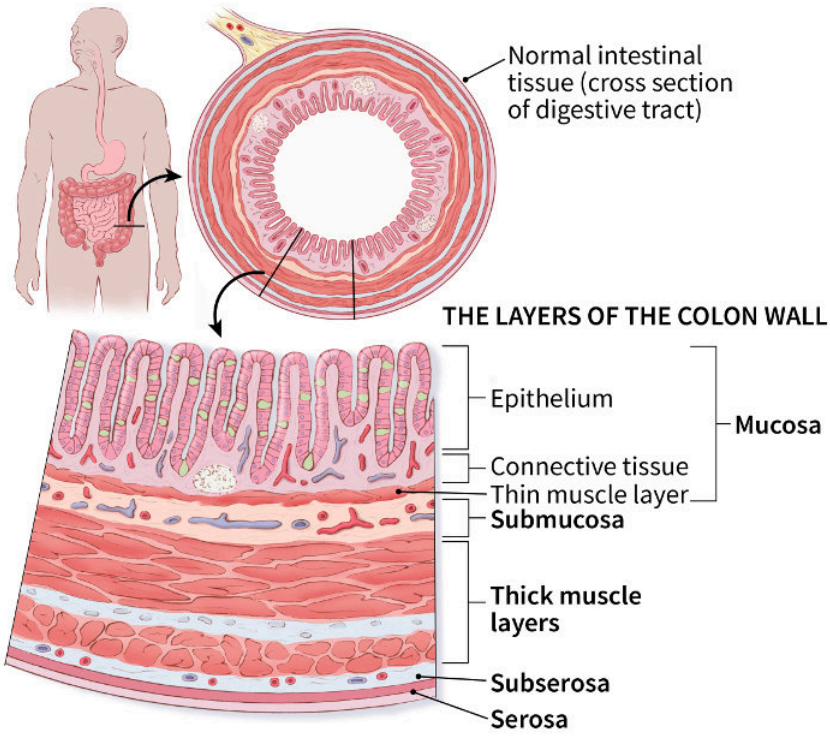

Figure 1. Cross section of the human colon with a magnification of the intestinal walls.[4]

1.2: Problems with Current Cancer Treatment

Cancer treatments vary by location of the cancer as well as the proximity to nearby vital organs. Most often, especially with late stage metastasized cancers, a systemic approach is required. Initially, this meant mass radiation of the body to target fast replicating cells. Radiation can kill fast replicating cells by irreparably damaging the DNA of the cell during the mitosis (M) phase of cell replication.[5] Unfortunately, radiation is not able to selectively target cancer above other fast-growing cells or cells in M phase of replication. As a result, cells that fall into these

categories are also targeted and begin apoptosis causing adverse side-effects in patients. As cancer treatment improved, so did the selectivity of the treatments. Radiation became more targeted and additional forms of treatment began to be developed such as immunotherapies and small-molecule targeted therapies.

Immunotherapies revolve around increasing the body's natural immune responses to better target cancer. These include immune checkpoint inhibitors, T-cell transfer, monoclonal antibodies, treatment vaccines and immune system modulators. The most commonly used methods either identify cancer cells to the immune system for destruction or strengthen the immune system allowing it to better fight the cancer. Despite this more selective approach immunotherapeutics still possess a number of difficulties. The first difficulty is cancer's ability to actively adapt to become resistant to the therapy, which is a common issue across many treatments. Second, immunotherapeutics are typically effective in only a subset of the patient population. Lastly, immunotherapeutics can also cause adverse immune affects by increasing the activity of the immune system causing it to attack normal cells.

Targeted therapies take advantage of specific aspects of cancer to cause destruction. These include marking the cancer for immune destruction, triggering apoptosis, or delivering toxins directly to the cancer cells. This treatment style has the benefit of being extremely selective as it is designed to target cancer specific traits. However, this treatment faces similar issues to others in that cancer can develop immunities to the treatment over time and each treatment can have its own side effects due to the broad range this class of treatments cover.

Most cancer treatment regiments require a combination of these treatments to ensure the patient is completely free of cancer. As such, side effects begin to increase as treatments

continue and selectivity goes down. As a result, a global search for treatments with high selectivity and low side effects is underway.

1.3: Prostaglandin Interactions within the Body

Prostaglandins are a class of lipid autacoids, or local hormones, and are derived from the compound arachidonic acid (AA). Prostaglandins play an important part in homeostatic regulation as well as the inflammatory response.[6] The four series of prostaglandins (PGE_2, PGI_2, PGD_2, $PGF_{2\alpha}$) are produced naturally throughout the body but often at a low concentration unless the local tissue is inflamed. Inflamed tissues will immediately start producing high levels of prostaglandins and tend to be a precursor to the arrival of leukocytes and higher immune response. This production begins when arachidonic acid is released from the lipid bilayer and metabolized by cyclooxygenases (COX) to form Prostaglandin H_2 (PGH_2). As seen in Figure 2, this includes a cyclization as well as the introduction of chirality to the molecule. The enzymatic metabolism of arachidonic acid can be blocked by non-steroidal anti-inflammatory drugs (NSAIDs) pointing to the efficacy of NSAIDs in pain and inflammatory regulation.

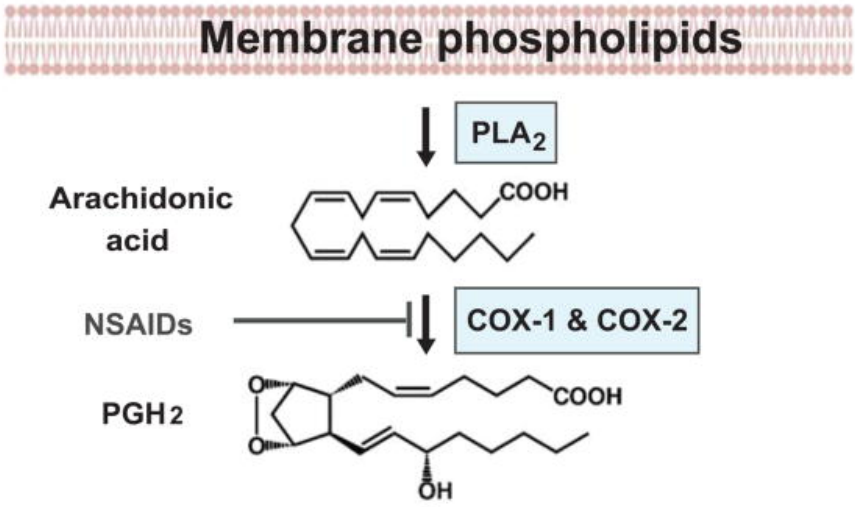

Figure 2. Enzymatic metabolism of arachidonic acid to central prostaglandin H_2

1.3.1: Interaction of D-Series Prostaglandins Within the Body

Prostaglandin D_2 (PGD_2) and its derivatives are produced in the central nervous system and associated tissues by metabolism of PGH_2 by Prostaglandin D Synthases (PGDS). D-series prostaglandins are responsible for both homeostatic regulation and inflammatory response with differing results based on location of synthesis.[7] For example, D-series prostaglandins are responsible for regulating sleep and pain reception when produced in brain tissue and when produced in immune cells assists in inflammatory response. D-series prostaglandins are able to be further metabolized into the J-subseries prostaglandins through a series of non-enzymatic dehydrations to produce 15d-$\Delta^{12,14}$-PGJ_2 as displayed in Figure 3.[8] The presence of albumin can assist in the production of Δ^{12}-PGJ_2.

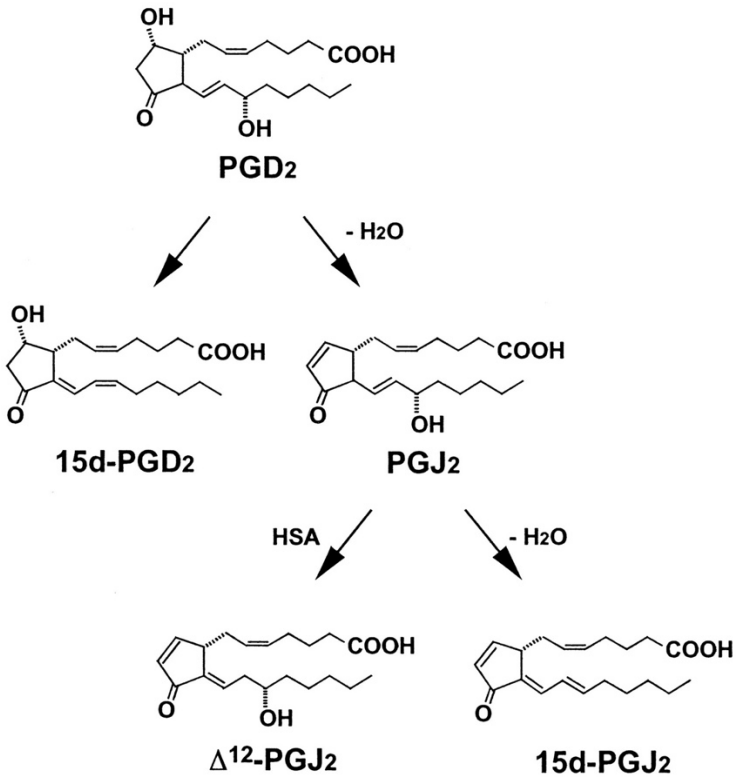

Figure 3. Metabolism of PGD_2 to 15d-$\Delta^{12,14}$-PGJ_2[8]

1.3.2: Interaction of Prostaglandins with Membrane Bound Receptors

Prostaglandins, across all series, interact with the cell through a seven membered trans-membrane protein receptor called G protein-coupled receptors (GPCRs). D-series prostaglandins specifically interact with GPCRs through the subtype PGD receptor 1 (DP1) and the chemoattractant receptor-homologous molecule expressed on T helper 2 (TH2) cells known as PGD receptor 2 (CRTH2 or DP2).[9]

1.4: Previous Prostaglandin Work

Initial studies on the anandamide (AEA) compound determined that the efficacy of AEA, the pre-metabolite to 15d-$\Delta^{12,14}$-PMJ_2, is both independent of cannabinoid receptors as well as dependent upon creating oxidative stress as it's mechanism of action.[10] As shown in Figure 4,

NMSC cells are treated with glutathione (NAC) or Trolox (a synthetic vitamin E analog, known for its antioxidant effects) for two hours and then treated with 20 μM AEA for one hour. (A higher absorbance indicates the presence of more living cells.) This study demonstrated that the cytotoxicity of AEA is partially reliant on oxidative stress. However, at high concentrations of NAC and Trolox there is still a significant amount of cell death as a result of AEA indicating an additional mechanism of cell death.

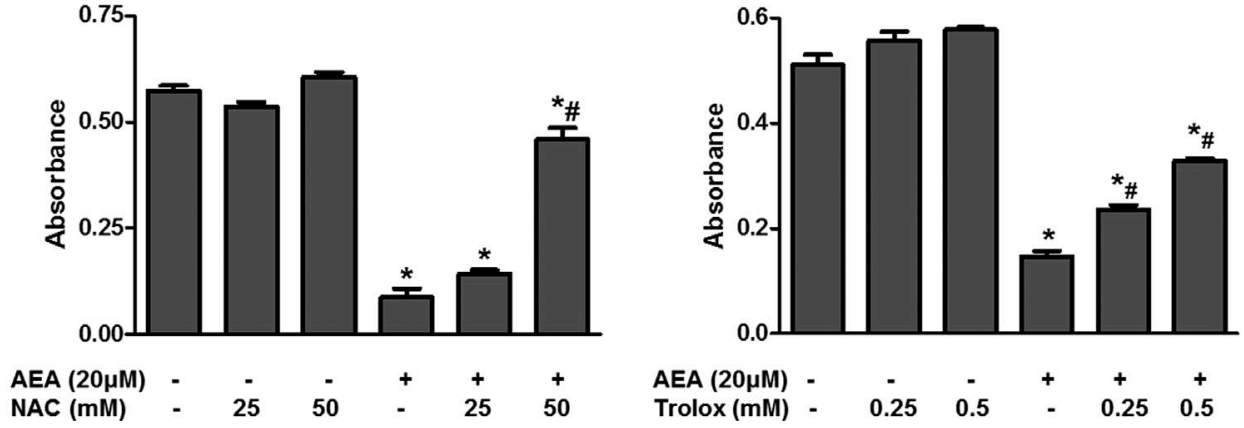

Figure 4. Cytotoxicity of AEA when applied to JWF2 cells treated with Glutathione and Trolox[10]

After establishing both the efficacy and a partial mechanism of AEA, the full mechanism of cell death needed to be determined. During this process the first instance of AEA being metabolized into 15d-$\Delta^{12,14}$-PMJ_2 was demonstrated. After a series of experiments, it was determined that AEA was metabolized by COX-2 and prostaglandin-D synthase (PGDS) as shown in Figure 5.

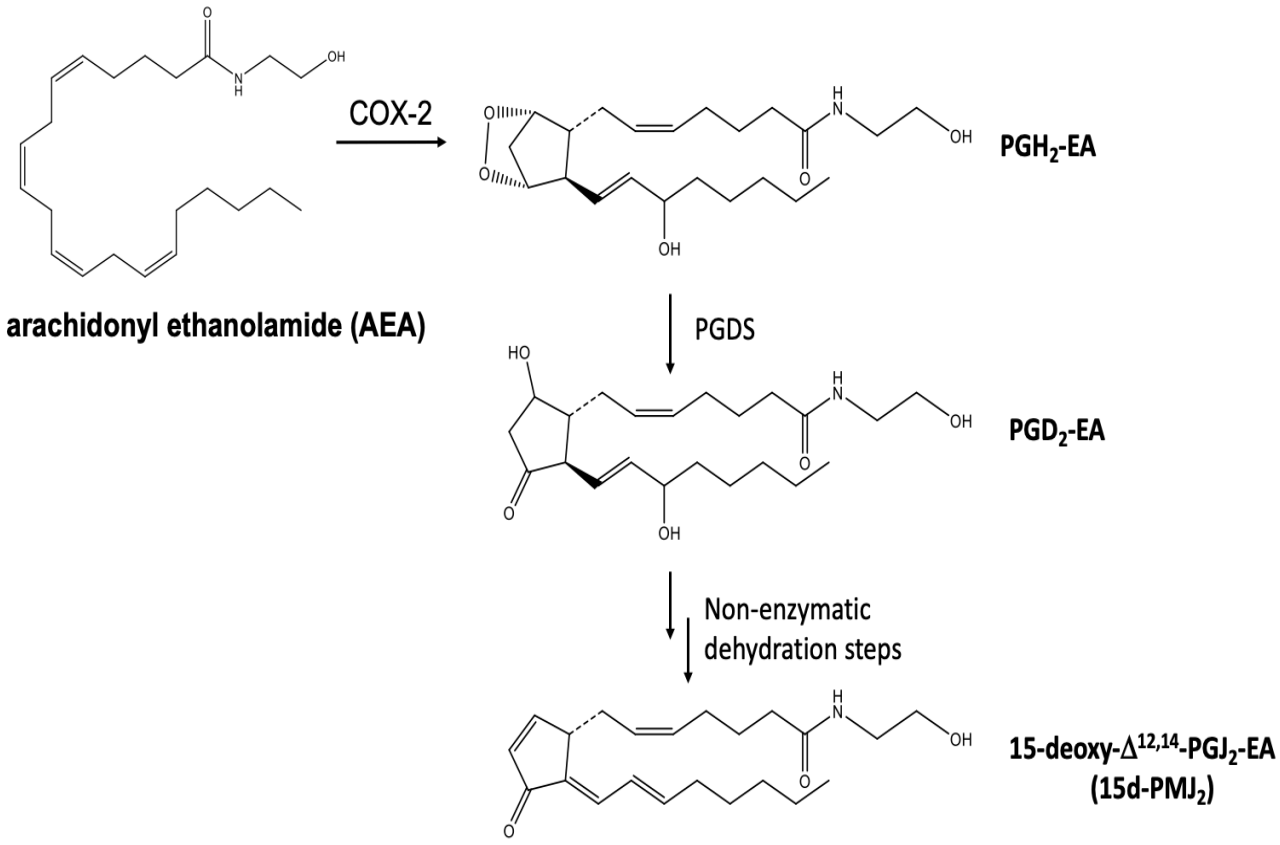

Figure 5. In vivo 15d-$\Delta^{12,14}$-PMJ_2 synthesis involving cyclooxygenase-2 (COX-2) and prostaglandin-D synthase (PGDS)

After discovery of 15d-$\Delta^{12,14}$-PMJ_2, studies began on the cytotoxicity of the metabolite. As shown in Figure 6, a much higher potency was noted in tumorigenic cancer cells while maintaining the selectivity necessary to still be a viable cancer treatment. With the introduction

of these results, new work began with a focus on solely the metabolite.

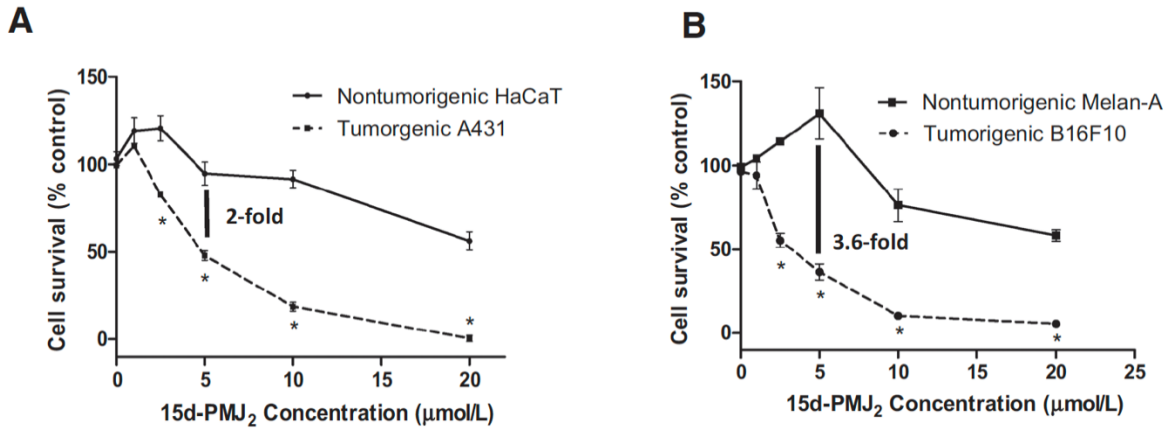

Figure 6. Cytotoxic Effects on Tumorigenic and Non-Tumorigenic (A) Human and (B) Murine Cells Lines to Demonstrate Selectivity

One such study determined that, while 15d-$\Delta^{12,14}$-PMJ_2 does cause oxidative stress, it is not reliant upon it to induce apoptosis unlike AEA.[11] Previous studies have demonstrated that 15d-$\Delta^{12,14}$-PMJ_2 is selectively cytotoxic to cancer cells by inducing endoplasmic reticulum stress that is capable of restarting the apoptosis pathway in cancer cells.[2]

1.4.1: AEA Derivatization

Due to the increase in selectivity and cytotoxicity of AEA and 15d-$\Delta^{12,14}$-PMJ_2 when compared to similar classes of cancer therapeutics a next generation of the treatment was proposed in order to increase efficacy. To this end, Dr. Andrew Morris developed several AEA derivatives, focusing on the functionalization of amide group, to test for increased cytotoxicity as shown in Figure 7.[12]

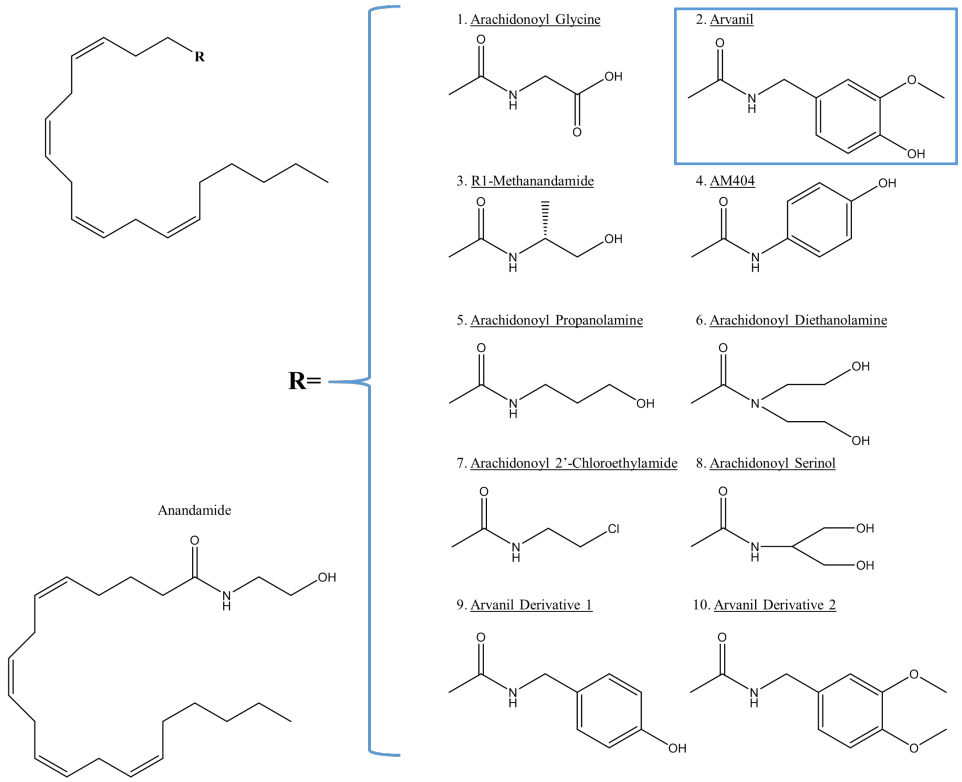

Figure 7. Derivatives of AEA[12]

Each derivative was tested via an MTS assay to determine cytotoxicity. The most potent of these AEA derivatives was Arvanil. In both murine (JWF2) and human (HCA-7) skin cancer cell lines Arvanil demonstrated 90% cell death almost a full order of magnitude greater than that of AEA, as seen in Figure 8. For comparison, AEA killed approximately 10% of JWF2 cells at 10 μM.[12]

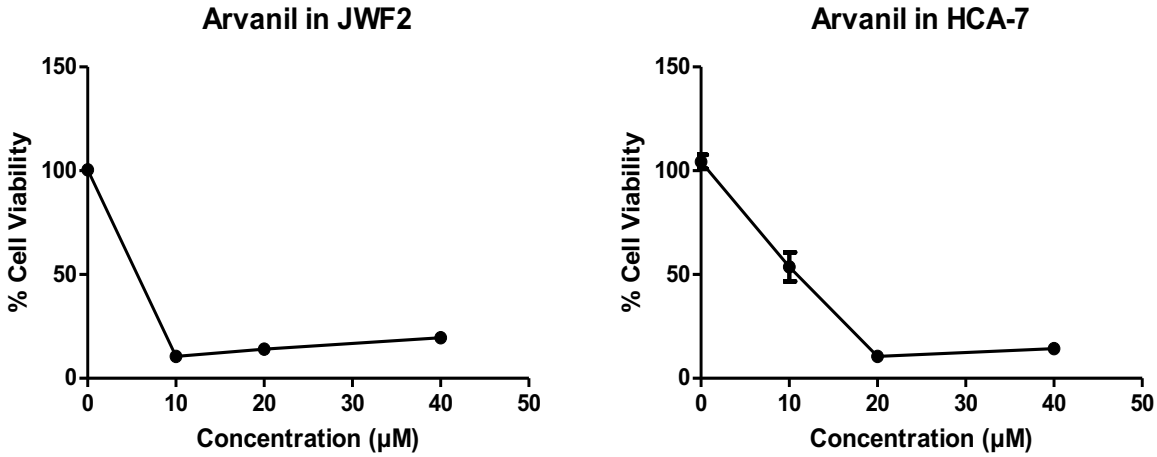

Figure 8. Cell Viability of Mouse (JWF2) and Human (HCA-7) Skin Cancer when Exposed to Arvanil

Based on previous results, it was hypothesized that Arvanil would be capable of undergoing a similar metabolism by COX-2 thus preserving the new functional group. The newly metabolized molecule 15d-$\Delta^{12,14}$-PMJ_2-Arvanil was later confirmed to be present in Arvanil treated COX-2 expressing cells by mass spectrometry.[1212]

Specific Aims

Arvanil and 15d-$\Delta^{12,14}$-PMJ_2-Arvanil are endocannabinoids and J-series prostamides respectively. Both molecules were determined to be the next likely candidates as Arvanil was shown to be more cytotoxic when compared to AEA as a result it is hypothesized that 15d-$\Delta^{12,14}$-PMJ_2-Arvanil should also be more cytotoxic. Much like AEA, Arvanil must be metabolized by the COX-2 enzyme that is overexpressed in colon cancer and non-melanoma skin cancer (NMSC) cells. In order to be metabolized by the COX-2 enzyme the concentration of Arvanil must saturate the available fatty acid amide hydrolase (FAAH) enzymes which disassembles the molecule into AA and the functional group vanillylamine. Once the available FAAH enzyme has been exhausted, metabolism by COX-2 enzyme can begin. Metabolism by COX-2 conserves the additional functional group and eventually results in the production of 15d-$\Delta^{12,14}$-PMJ_2-Arvanil through the same mechanism shown in Figure 5.

The ability to bypass the metabolism steps to produce 15d-$\Delta^{12,14}$-PMJ_2-arvanil should result in a lower concentration necessary to produce the same effect as the metabolite no longer has to saturate available FAAH enzyme to be metabolized to the active drug.

Specific Aim 1: Synthesize and determine cytotoxicity of Arvanil in CT-26 and HCA-7 cells compared to AEA.

It has been demonstrated in previous studies that the addition of an ethanolamine functional group to AA produces AEA, which has a selective cytotoxic effect on cancer cell. Previous work also identified Arvanil as a potential next generation drug with a higher potency. Arvanil was chosen for its potential to resist degradation by FAAH, and preliminary data showed that it would have similar or higher cytotoxicity compared to AEA.[13] Previous work also

indicated that the COX-2 metabolism would similarly conserve the new functional group during the transformation to a J-series prostaglandin.

The synthesis and purification protocols of Arvanil were streamlined to produce a high yield of pure product. After purification, Arvanil was characterized, and a protocol was developed for dosing both CT-26 and HCA-7 cells.

Specific Aim 2: Synthesize and determine cytotoxicity of 15d-$\Delta^{12,14}$-PMJ_2-Arvanil in CT-26 and HCA-7 cell lines to compare to 15d-$\Delta^{12,14}$-PMJ_2 activity.

Based on previous studies, it has been established that the pre-metabolite anandamides AEA and Arvanil are metabolized to J-series prostamides that conserve the added functional groups.[12] As a result, it can be concluded that the increase in potency will be seen in Arvanil to 15d-$\Delta^{12,14}$-PMJ_2-Arvanil as was seen in AEA to 15d-$\Delta^{12,14}$-PMJ_2.

The synthesis protocol of 15d-$\Delta^{12,14}$-PMJ_2 was adjusted to circumvent the effects of the hydrochloride salt the new functional group, vanillylamine, introduces. After purification, 15d-$\Delta^{12,14}$-PMJ_2-Arvanil was characterized, and a protocol was developed for dosing both CT-26 and HCA-7 cells.

Specific Aim 3: Prepare micelles for drug transportation and determine effect on drug efficacy.

Thus far, 15d-$\Delta^{12,14}$-PMJ_2 has only been tested in vivo on mice by intralesional injection for melanoma skin cancer. Experimental data from previous studies has demonstrated activity against several different cancer cell lines, including colorectal cancer. However, use of 15d-$\Delta^{12,14}$-PMJ_2 against these cancers, especially in the form of intravenous delivery, may be limited

due to the poor aqueous solubility of 15d-$\Delta^{12,14}$-PMJ_2 and may also be neutralized by glutathione. Further, its lipophilic profile may lead to adipose tissue sequestration. Polymeric micelles are well suited for drug delivery purposes and have been shown to aid in drug targeting to tumor tissue, prolong drug circulation time, and enhance accumulation of the drug at the tumor site. Collectively, this behavior of supramolecular assemblies is referred to as the enhanced permeability and retention effect (EPR effect).

In this study, a modified protocol for micelle formation will be developed in order to deliver the hydrophobic drugs; AEA, Arvanil, 15d-$\Delta^{12,14}$-PMJ_2 and 15d-$\Delta^{12,14}$-PMJ_2-Arvanil. The micelles, made of a 1:6.5 DSPE: TPGS, will be initially characterized by fluorescence to determine critical micelle concentration (CMC) and will be tested on HCA-7 cell lines to determine the effect of the micelles on drug efficacy by comparing to previously published MTS cell viability data.

Chapter 2: Materials and Methods

2.1: Synthesis Reagents

Arachidonic acid was purchased from NuChek Prep (Elysian, MN). Ethanolamine, acetonitrile, O-(benzotriazol-1-yl)-N,N,N',N'-tetramethyluronium tetrafluoroborate (TBTU), and N,N-diisopropylethylamine (DIPEA) were purchased from Sigma-Aldrich (St. Louis, MO). 15d-$\Delta^{12,14}$-PGJ_2 was purchased from Cayman Chemical Company (Ann Arbor, MI) 4-Hydroxy-3-methoxy-benzylamine hydrochloride (vanillylamine) was purchased from Millipore Corporation (Billerica, MA).

2.2: Synthesis, Purification and Characterization of Arvanil and 15d-$\Delta^{12,14}$-PMJ_2-Arvanil

The general synthetic model for both Arvanil and 15d-$\Delta^{12,14}$-PMJ_2-Arvanil are displayed in Figure 9. The starting compound, either AA or 15d-$\Delta^{12,14}$-PGJ_2, are added to the reaction flask with 1.3 molar equivalences of TBTU and 2 equivalences of DIPEA along with 2 mL of acetonitrile. The solution is allowed to mix for 5 minutes with stirring to deprotonate the terminal carboxylic acid. After this, 2 molar equivalences of vanillylamine are added to the reaction flask. The flask is sealed and placed under positive pressure with nitrogen gas and allowed to react for 2 hours.

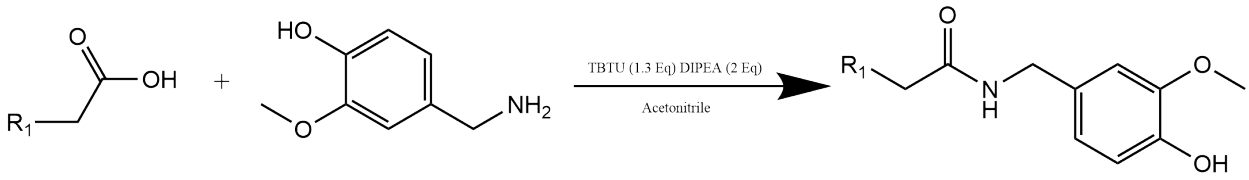

Figure 9. Generalized Reaction Scheme for Amide Bond Formation with Vanillylamine

2.2.1: Purification

After the reaction has completed, the contents of the flask are added to a separatory and the flask is rinsed with both diethyl ether and 18.2 MΩ-cm water. The separatory funnel is swirled gently for thirty seconds, and the water layer is drained. The addition of super-saturated sodium chloride solution is often required to resolve emulsions. This process is repeated an additional two times with the water layer being replaced each time. The recovered ether layer is allowed to evaporate naturally and resuspended in approximately 2 mL of ether and delivered to a sterilized one-dram vial.

If it is determined, through NMR characterization, that initial purification is necessary a liquid chromatography column may be used. The reaction mixture is loaded onto a silica column and rinsed with several milliliters of dichloromethane (DCM). Afterwards the column is rinsed with 100 milliliters of a 1:25 Methanol: DCM mixture that is capable of eluting a single band of product.

2.2.2 Characterization

Initial characterization of both molecules was accomplished using ^{1}H-NMR on a Bruker 400 MHz NMR as shown in both Figure 10 and Figure 11. Additional ^{13}C-NMR was performed when concentration permits.

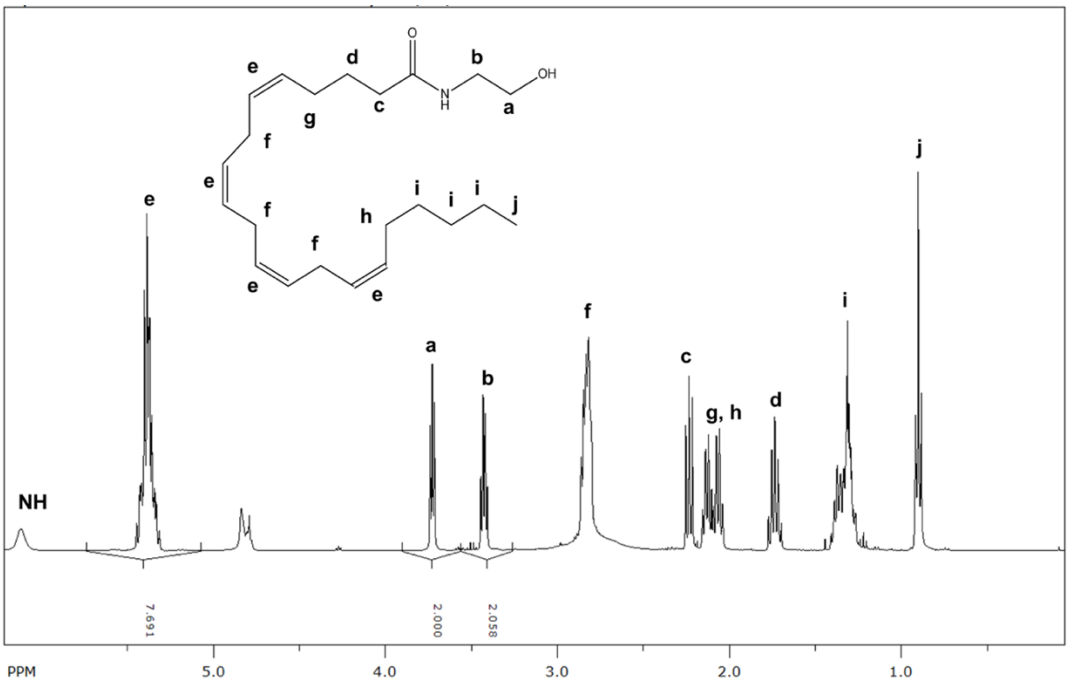

Figure 10. Assigned Proton NMR Spectrum of Arachidonic Ethanolamide (AEA)

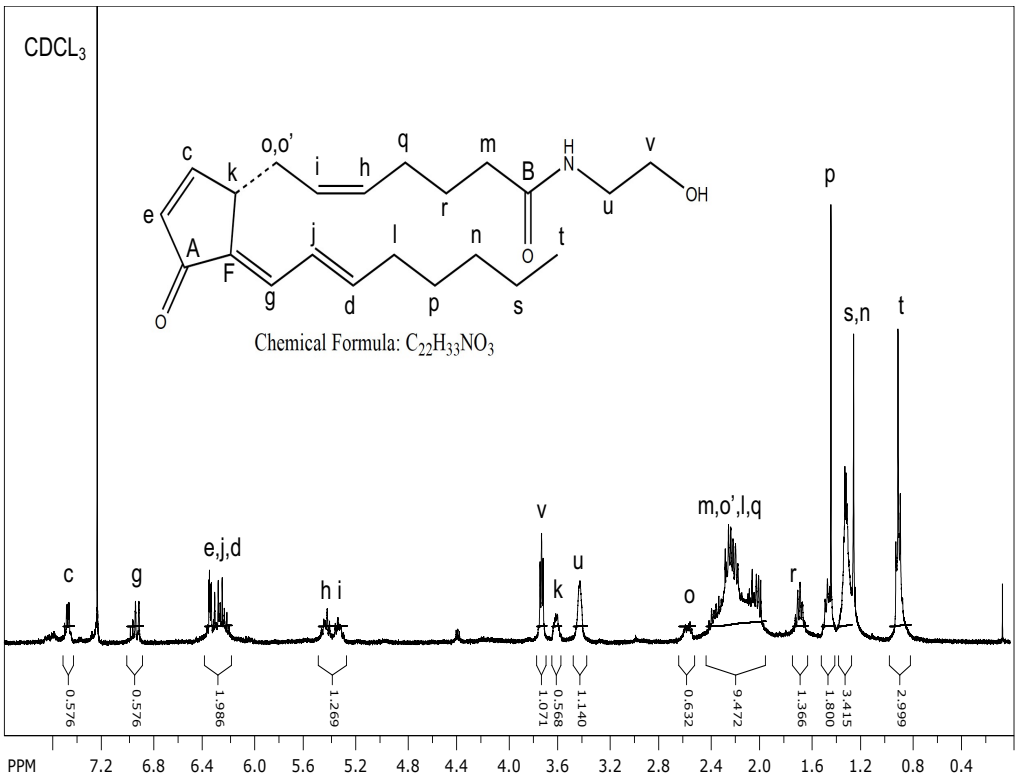

Figure 11. Assigned Proton NMR Spectrum of 15d-$\Delta^{12,14}$-PMJ$_2$ in $CDCl_2$

2.3: Cell Culture

HCA-7 human colorectal cancer cell line (Sigma-Aldrich, St. Louis, MO) were cultured in Dulbecco's Minimal Essential Media (DMEM) (Invitrogen) containing 10% heat-inactivated FBS, 100 mg/mL penicillin, 100 mg/mL streptomycin, and 1mM sodium pyruvate. CT-26 murine colorectal cancer cell line (Thermo Fisher Scientific, Waltham, MA) was cultured in Roswell Park Memorial Institute (RPMI) 1640 Medium (Gibco) containing 10% heat-inactivated FBS, 100 mg/mL penicillin, 100 mg/mL streptomycin, and 1mM sodium pyruvate.

2.4: MTS Cell Viability Assays

Cells were plated in 96-well plates and cultured for 48 hours until ~80% confluency was achieved, and complete media is removed. Serum-free media containing a range of concentrations appropriate to each compound or delivery system are added and allowed to react for 24 hours (CT-26) and 48 hours (HCA-7). A 20 μL aliquot of MTS reagent (Promega, Madison, WI) was added to each well as described by manufacturer and the absorbance was measured at 495 nm. Presented data is shown as mean ± standard error of mean.

2.5: Micelle Formation

Micelles were prepared from mixture of two polyethylene glycol-modified lipophilic compounds, 1,2-distearoyl-sn-glycero-3-phosphoethanolamine-N-[methoxy(polyethylene glycol)-2000] (DSPE-PEG2000) and D-α-tocopherol polyethylene glycol 1000 succinate (TPGS). Both compounds have been used for anti-cancer drug delivery in cell and animal studies and are employed in FDA approved drug formulations.[14,15] A 1:5 mole ratio of DSPE-PEG2000: TPGS was used in all micelle preparations; these were prepared as solutions in ethanol where the appropriate amount of drug molecule, dissolved in ethanol, was added. All micelle and micelle

drug solutions were prepared by thin film casting in a volumetric flask followed by the addition of water or aqueous buffer. The solutions were then sonicated at 37°C for 30 minutes and then allowed to cool to room temperature before use.

2.6: CMC Measurement

The critical micellar concentration (CMC) of the DSPE-PEG2000: TPGS formulation was estimated by the fluorescence spectroscopy, using pyrene as the probe. All measurements were made on a PTI fluorescence spectrometer in a 1 cm quartz cuvette. A series of 9 solutions were made (10 mL or 100 mL volumes) in volumetric flasks by the method discussed in section 2.4, where the micelle concentrations were 0.3132, 0.09918, 0.04959, 0.03132, 0.009918, 0.004959, 0.0024795, 0.0004959, and 0.000783 mg/mL. Each solution contained 1 mM pyrene which was added in acetone followed by evaporation prior to the addition of the lipid solution.[15,16]

2.7: Micelle Characterization

In order to determine the structure of the unloaded micelles a scanning electron microscope (SEM) was used. The SEM samples were prepared by dusting the lyophilized micellar powder on to double-adhesive conductive tape, which had been applied previously to a copper stub, and coated with a 30 nm thin layer of gold/palladium. After preparation, the stubs were scanned by Dr. Silvana Pasetto, Department of Biology using a FEI Quanta 200 Variable pressure Scanning Electron Microscope.

Chapter 3: Synthesis and Cytotoxic Evaluation of Arvanil and 15d-$\Delta^{12,14}$-PMJ_2-Arvanil

3.1: Experimental Design

Previously it has been established that the AEA is metabolized by COX-2, after overwhelming the capabilities of FAAH, to a J-series prostaglandin that conserves the new ethanolamine functional group. The prostaglandin, when directly introduced, sees an increase in potency as it no longer needs to overcome FAAH and be metabolized by COX-2 to get to a cytotoxic form. The prostaglandin also does not rely on oxidative stress unlike anandamide. Previous studies have also indicated that new functional groups could replace the ethanolamine to increase cytotoxicity without negatively effecting the cytotoxicity that results from adjusting the double bond (pharmacophore) region.[2,12] One such group is vanillylamine as shown below.

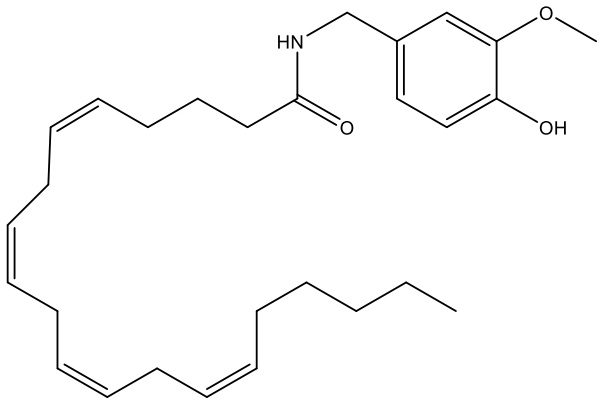

Figure 12. Chemical structure of Arvanil

Initial studies indicate that the replacement of ethanolamine with vanillylamine to form Arvanil (Figure 12) would result in a higher cytotoxicity and was predicted to see a similar scaling of cytotoxicity seen from AEA to 15d-$\Delta^{12,14}$-PMJ_2.

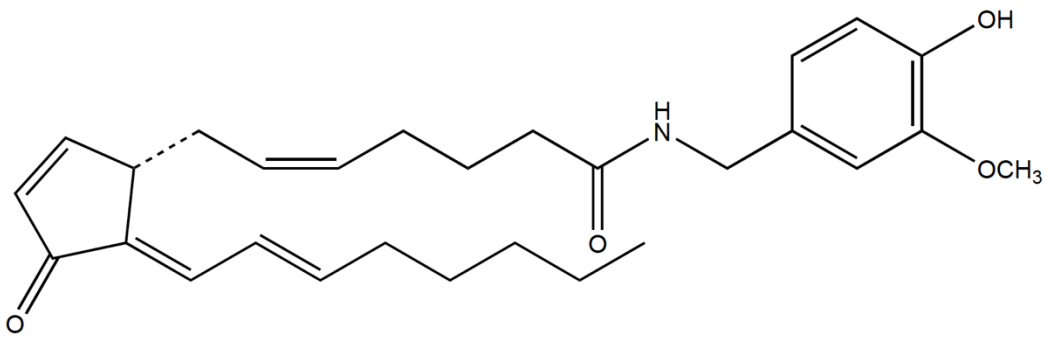

Figure 13. Chemical Structure of 15d-$\Delta^{12,14}$-PMJ_2-Arvanil

The intent of this investigation is to determine the cytotoxicity of Arvanil and J-series prostaglandin metabolite 15d-$\Delta^{12,14}$-PMJ_2-Arvanil (Figure 13) in murine (CT-26) and human (HCA-7) colorectal cancer. These studies necessitate the synthesis of both Arvanil and 15d-$\Delta^{12,14}$-PMJ_2-Arvanil as well as the purification and characterization discussed in Chapter 2.

3.2 Cytotoxicity of Arvanil in CT-26 Cells

In order to determine the cytotoxicity of Arvanil (ARV), CT-26 mouse colon cancer cells were treated with six different concentrations of drug (2.5, 5, 25, 50, 100, and 200 μmol/L) and cell viability was measured by MTS assay performed in triplicate. The cytotoxicity was compared to that of the prodrug, arachidonoyl ethanolamide (AEA). The arachidonoyl ethanolamide compound was used as a control because the efficacy was established in previous studies. At 25 μmol/L, Arvanil reduced the cell viability by 90% whereas at the same concentration arachidonoyl ethanolamide had no measurable effect on cell viability (i.e., it was indistinguishable from the control). Thus, Arvanil is more potent than arachidonoyl ethanolamide. Based on the previous studies of AEA and the metabolized drug, 15d-$\Delta^{12,14}$-PMJ_2, it was inferred that the Arvanil prodrug would show a similar ratio of efficacy compared to the

application of its corresponding metabolite. This would potentially result in a much more potent drug when metabolized to 15d-$\Delta^{12,14}$-PMJ_2-arvanil.

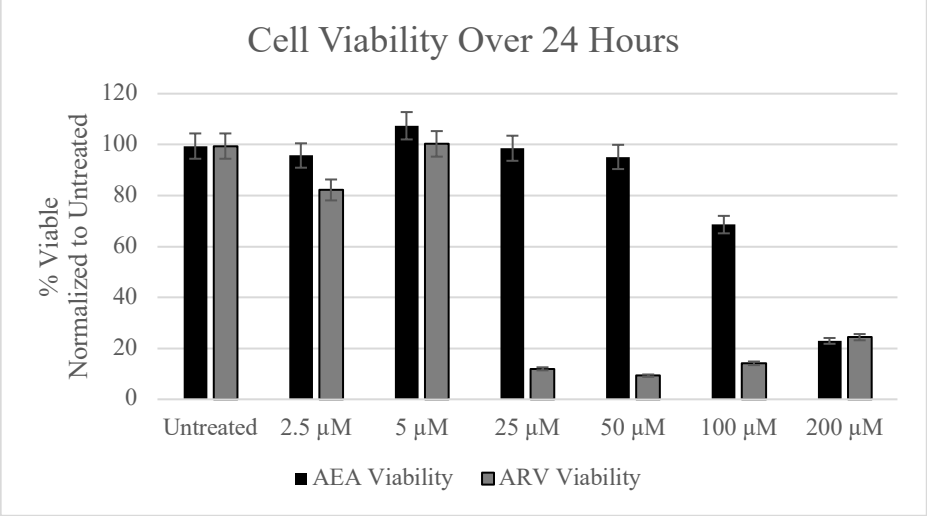

Figure 14. Cell Viability Study of AEA and Arvanil in CT-26 cells

3.3 Cytotoxicity of 15d-$\Delta^{12,14}$-PMJ_2-Arvanil in HCA-7 Cells

In order to determine the cytotoxicity of 15d-$\Delta^{12,14}$-PMJ_2-arvanil (PMJ-ARV), HCA-7 primary human melanoma cells were treated with different concentrations of drug (1.0-10 µmol/L) and cell viability was measured by MTS assay performed in triplicate. The cytotoxicity was compared to that of the metabolized product 15d-$\Delta^{12,14}$-PMJ_2 (PMJ). The 15d-$\Delta^{12,14}$-PMJ_2 compound was chosen as a control based on previously established efficacy studies. With exception of 1 µM and 10 µM, 15d-$\Delta^{12,14}$-PMJ_2-arvanil was indistinguishable from the vehicle. At 1 µM, 15d-$\Delta^{12,14}$-PMJ_2-arvanil was mildly more cytotoxic than 15d-$\Delta^{12,14}$-PMJ_2. However, at 10 µM, 15d-$\Delta^{12,14}$-PMJ_2-arvanil was approximately a third as cytotoxic when compared to 15d-$\Delta^{12,14}$-PMJ_2 at the same concentration. It is currently theorized that the bulkier functional group

is preventing entry into the cell thereby preventing the molecule from reaching its intracellular target.

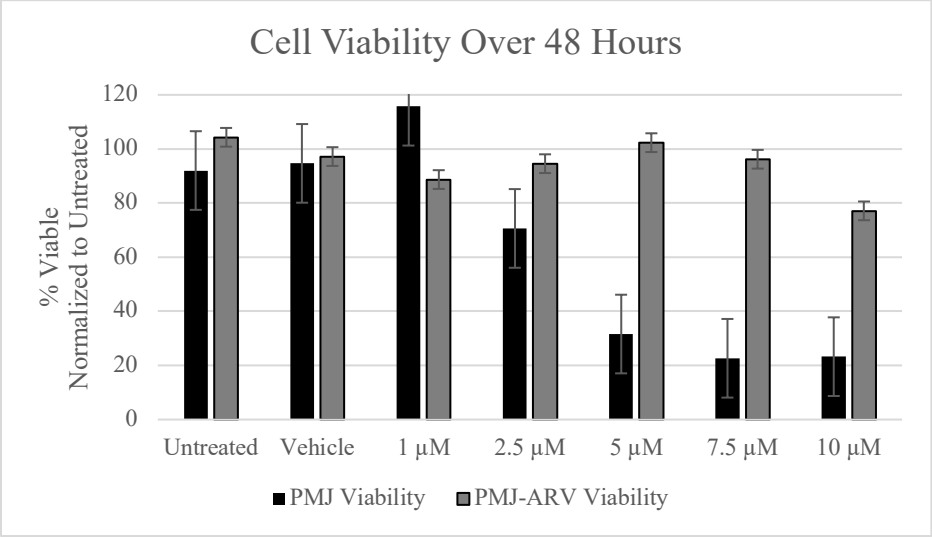

Figure 15. Cell Viability of 15d-$\Delta^{12,14}$-PMJ_2 and 15d-$\Delta^{12,14}$-PMJ_2-Arvanil in HCA-7 cells

Chapter 4: Drug Delivery

4.1: Micelles as Drug Delivery

A micelle is a nano-scale supramolecular structure that is composed of molecules with a hydrophobic and hydrophilic portion to each polymer unit. Similar to the phospholipid membrane of eukaryotes, the polymer units will spontaneously form a micelle when above the critical micelle concentration (CMC). At or above the CMC, the micelles will maintain a thermodynamic equilibrium exchanging polymer units with the solution around the micelle but maintaining the micelle. Below the CMC, the micelles will become unstable and will begin to disassemble over time.[17] The rate of this disassembly is described by the kinetic stability of the micelle preparation. The CMC of each micelle will change depending on the formulation of the micelle, solution the micelles are suspended in, and the amount or type of drug being loaded into the micelle. The lower the CMC for a specific formulation the more stable the micelle will be. One formulation that is commonly used is the introduction of polyethylene glycol (PEG) subunits to the polymer units. PEGylating the micelles can lower the CMC by several orders of magnitude and has been shown to also increase the kinetic stability of the micelle when below the CMC. When above the CMC and in the presence of a hydrophobic molecule, such as a drug, the micelle will form around the molecule and encase it as seen in Figure 16. This will allow for the transportation of the molecule in aqueous environments.

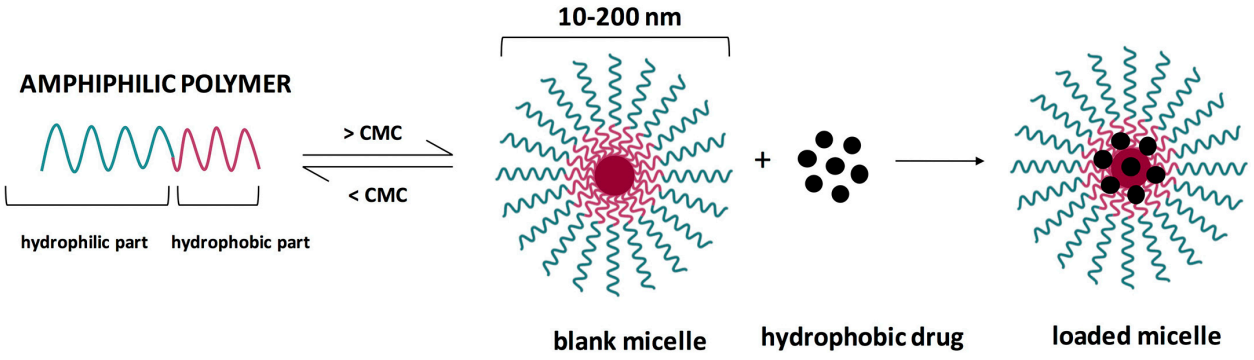

Figure 16. Representation of micelle formation around a hydrophobic drug[17]

For the purpose of drug delivery, the aqueous environment is often the blood stream. For many hydrophobic drugs, the limitation to use is the ability to introduce a high enough concentration of soluble drug to be effective, while others face neutralization by the body's natural defenses. Micelles are capable of providing a solution to both. Due to micelle's ability to store hydrophobic drugs within or close to its hydrophobic interior the drugs are able to move throughout the blood stream and be delivered to their targets without direct injection to the tumor site. Additionally, and especially important for anandamides and J-series prostaglandins, the micelles provide protection from extracellular glutathione as the drug itself is housed within micelle until it is released.

After the drugs (anandamides or J-series prostaglandins) have been loaded into the micelles and the micelles have been introduced to the blood stream they are expected to travel to and aggregate in tumors due to their naturally porous vascular system. This system is a result of angiogenesis, rapid vascularization triggered by tumor cells to provide resources and infrastructure for continued growth. Due to the nano-scale nature of the micelles, they are able to slip through new blood vessels and aggregate at the tumor site preferentially over other tissues.[17]

The micelles, after successfully arriving at the target site, have three possible methods to introduce the drug to the cell as can be seen in Figure 17. The first is the slow release of the drug which occurs naturally over the lifetime of the micelle. The second is complete micellular disassembly, this commonly results from the micelles concentration dipping below the CMC and tending towards kinetic equilibrium. The third method is intact penetration where the micelle along with the drug are endocytosed into the cell itself.

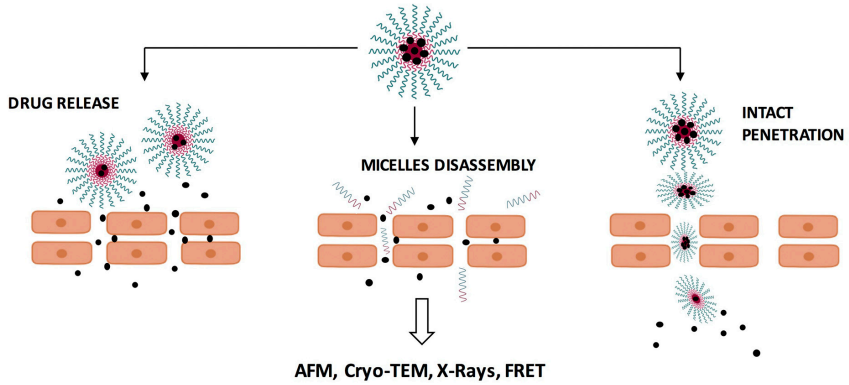

Figure 17. Representation of drug release from micelles in a biological system[17]

While capable of all three methods, micelles tend to be endocytosed as opposed to disassembly or drug release. One benefit that is gained from endocytosis is the of ability of specific types of polymer units, after internalization, to prevent the use of drug efflux pumps and thereby limiting cancer's ability to develop multi-drug resistances.[17] One of these polymer units is D-α-Tocopheryl Polyethylene Glycol 1000 Succinate (TPGS).

4.2: Micelle Formation

The micelles were made from a 1:5 ratio of 1,2-Distearoyl-sn-glycero-3-phosphoethanolamine (DSPE) and TPGS using a modified method from the Zhang (2019).[15] Instead of adding an ethanol solution of the drug to an aqueous solution of the micelle forming

components followed by dialysis to remove the ethanol, the drug was added along with appropriate concentrations of DSPE and TPGS in an organic solvent to a flask and form a thin film either by drying under a stream of nitrogen gas or under reduced pressure. The film was rehydrated in a PBS solution (pH 7.2), and the solution sonicated at 37 °C for 30 minutes. Studies were performed, at earliest, only after the micelle solutions were allowed to cool to room temperature.

Initial studies were performed to determine the critical micelle concentration (CMC) of these micelles using pyrene as the encapsulated fluorescent marker. The CMC serves as a measure of micelle stability as micelles disassemble at concentrations below this value. The lower the CMC value of a micelle preparation, the greater the predicted stability of the micelle particles. Figure 18 shows a sample measurement where the CMC of the micelle preparation was estimated as the cross-point of the extrapolated intensity values of the low and high concentration regions. In this plot, the crossing point occurs at 0.0068 mg/mL and compares well to that of 0.0072 mg/mL reported by Zhang et al for 1:6.5 DSPE: TPGS micelles prepared in water.[15]

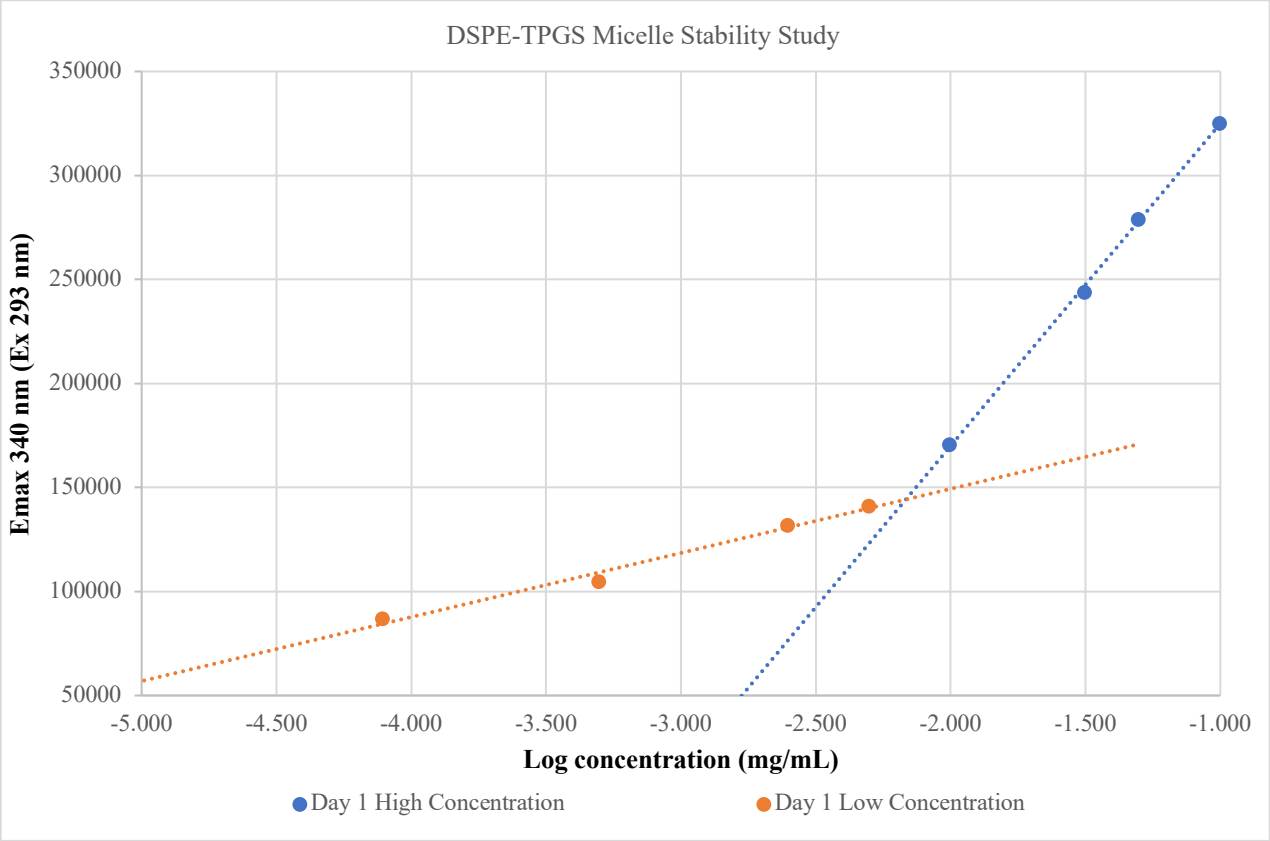

Figure 18. CMC determination of DSPE: TPGS micelles using fluorimetry with a pyrene indicator

The same set of micelle solutions used to produce Figure 18 were measured 2 and 15 days after preparation to determine their stability over time (Figure 19 and Table 1). CMC values at these later time points were found to vary less than an order of magnitude from the initial value measured on day 1 (CMCs = 0.0061 and 0.0042 mg/mL, respectively). The apparent change in CMC value appears to be primarily caused by a lowering of the slope of the low concentration data points. Since these micelles solutions should be below the CMC they are expected to disassemble, thus releasing the pyrene into aqueous solution with a concomitant lowering of the pyrene fluorescent emission intensity. By day 15, there is a lowering of the slope

of the high concentration data points demonstrating a slow loss of the encapsulated pyrene, possibly by micelle disassembly.

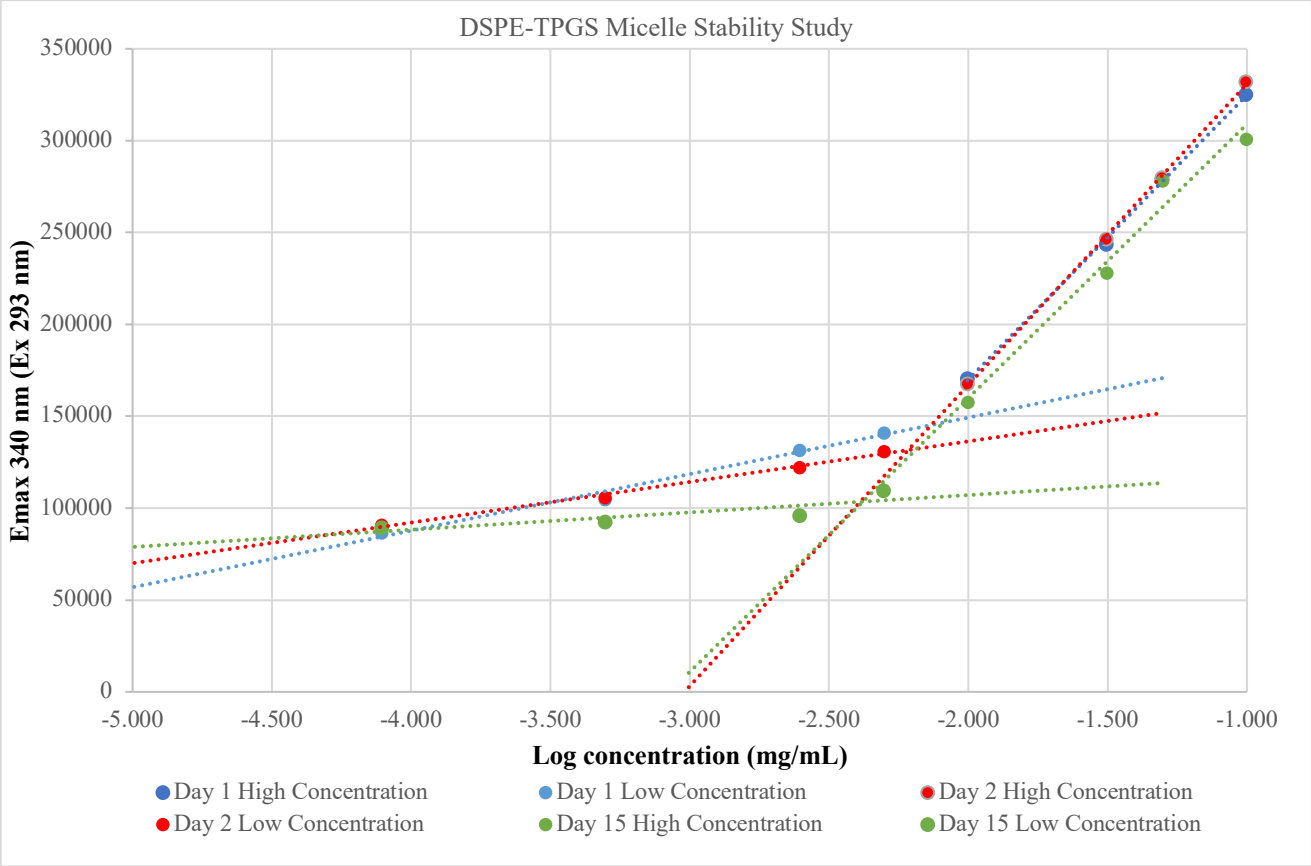

Figure 19. DSPE-TPGS micelle stability study

Table 1. Comparison of stability study CMC

	Day 1	Day 2	Day 15
High Concentration	y = 154961x + 479904	y = 163919x + 494909	y = 149084x + 458133
Low Concentration	y = 30802x + 210938	y = 22121x + 180626	y = 9412.7x + 125936
Calculated CMC	0.0068 mg/mL	0.0061 mg/mL	0.0042 mg/mL
Difference from Day 1	-	-0.0007 mg/mL	-0.0026 mg/mL

4.3: Characterization of Micelles

In order to confirm the 1:5 DSPE: TPGS micelles are forming appropriately, a SEM image was taken (Figure 20) and compared to the literature (Figure 21) to determine the shape of the micelles.[18]

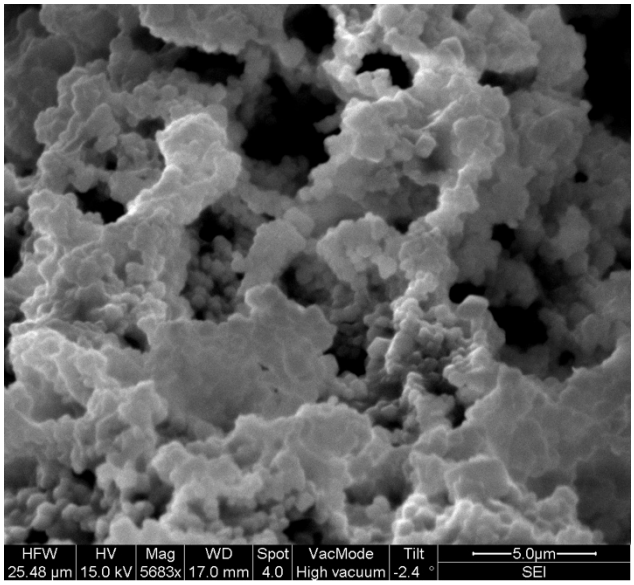

Figure 20. SEM Image of Unloaded Micelles

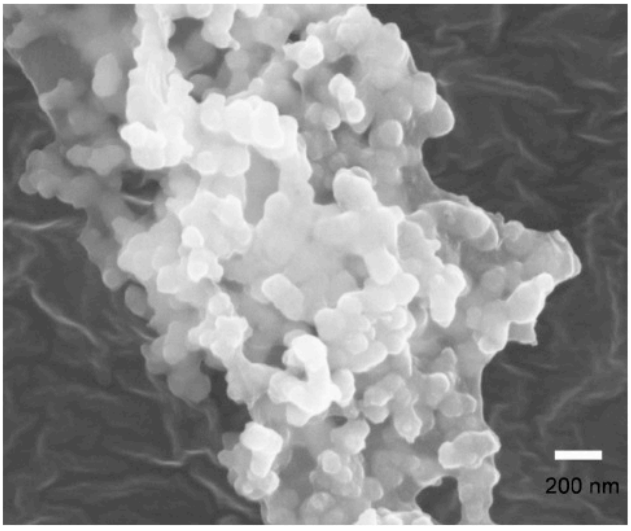

Figure 21. Literature SEM Image of Unloaded Micelles[18]

As can be seen in Figure 20 and Figure 21, each individual polyp is a complete micelle. Current instrumentation limits prevent the resolution seen in the literature. However, when taking into account scaling along with the additional 60 nm of gold/platinum present on the literature micelles, both the shape and size of experimental micelles are consistent with literature micelles. Further tests are planned to increase resolution as well as reduce micellar concentration to better isolate individual micelles for measurement.

4.4: Effect of Empty Micelles

In order to determine the effects of the 1:5 DSPE: TPGS micelles on the cells, a cell viability study was run in triplicate using the HCA-7 cell line. Micelles of different concentrations were prepared as stated in section 4.2; however, no marker or drug was encapsulated, thus these are called “empty micelles”. The micelles were rehydrated in a PBS solution (pH 7.2). To preserve the normal level of nutrients being delivered to the cells a concentrated (5x DMEM) media was prepared and the micelles were delivered for treatment in a 1:5 ratio of DMEM: micelle solution. For normalization purposes, both the untreated and the vehicle were in a solution of 1:5 5x DMEM: PBS. Cells were treated for 48 hours, and an MTS assay was performed at the end of the treatment period.

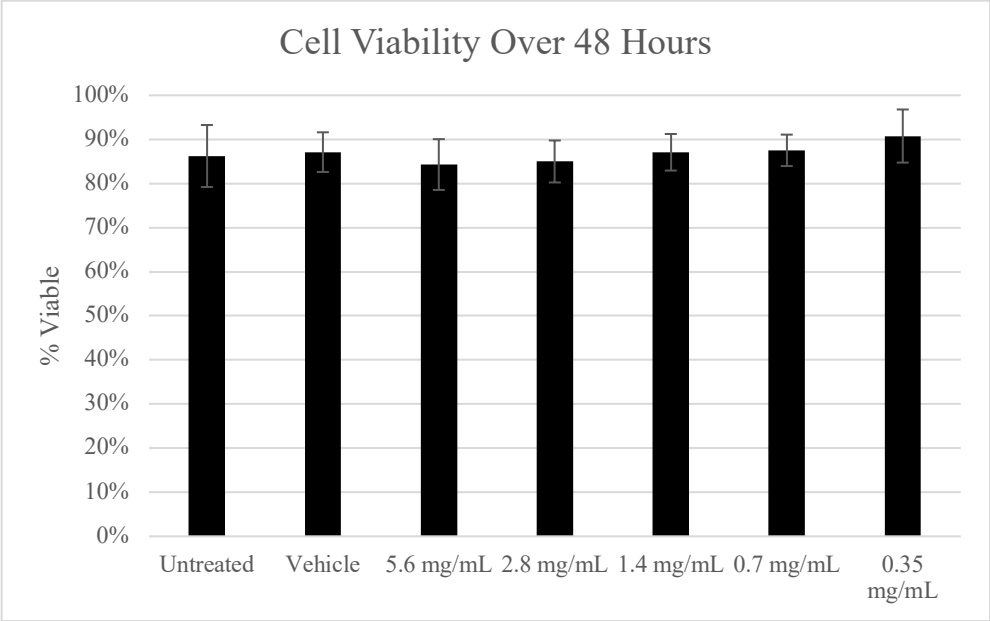

Figure 22. Cell Viability of Empty Micelles in HCA-7 Cells

As can be seen in Figure 22, the micelles did not have any significant effect on cell viability even at the extreme concentration of 5.6 mg/mL. This indicates that the micelles themselves will not have any effect on cell viability as the highest concentration of micelle achieved at any drug concentration is below 2.6 mg/mL based on the target of maintaining the drug: micelle ratio at or below 1:7.

4.5: Effect of Micelles on Drug Efficacy

After confirming the 1:5 DSPE: TPGS micelles were not capable of causing cell death at any concentration planned for in vitro or in vivo use, cell studies on loaded micelles were performed to determine if the current formulation was capable of providing similar or improved results compared to the drug alone. Micelles were prepared as stated in section 4.2 with varying concentrations of Arvanil (100 µM, 50 µM, 25 µM, 5 µM and 2.5 µM) with a standard concentration of 2.6 mg/mL of micelle. This maintains a drug: micelle ratio where the highest is

1:7 ratio at the highest drug concentration (100 μM). At drug concentrations below 100 μM, the ratio of micelle increases (e.g., at a 50 μM concentration of drug, the ratio is 1:14). Initial results (not shown) indicate no effect when compared to untreated and vehicle. It is currently theorized that the 48-hour treatment period is not an appropriate amount of time for the micelles to release the drug at any considerable concentration in that period. This is likely due to the concentration of micelles on the cell plate being much higher than the CMC.

Chapter 5: Review of Major Findings and Discussion

One next-generation drug molecule and its metabolite were noted in previous studies to have potential to show an increase in potency from AEA and 15d-$\Delta^{12,14}$-PMJ_2.[12] In this study Arvanil and 15d-$\Delta^{12,14}$-PMJ_2-Arvanil were synthesized, characterized and the cytotoxicity determined. Additionally, a protocol for micellular drug delivery was established including the synthesis protocol, characterization, and the cytotoxic effects of the micelles along with their effects on drug cytotoxicity.

5.1: Synthesis, Characterization Arvanil and 15d-$\Delta^{12,14}$-PMJ_2-Arvanil

The first goal of the study was to develop a protocol for the synthesis of Arvanil and 15d-$\Delta^{12,14}$-PMJ_2-Arvanil. Using the framework shown in Figure 9, idealized reaction times and equivalences were determined based on the new functional group vanillylamine. An adjustment was made to move away from reverse-phase HPLC as this resulted in a large percentage of product lost. It has been determined that the loss may result from quantity limitations. High loading of HPLC columns results in lower resolution, this may result in the loss of product during the collection of each peak. To combat this issue, liquid-liquid extraction is done using diethyl ether and distilled water with the option to run a column based on purity. The finalized reaction protocol produces ~95% raw yield and ~85% yield after purification due to loss during the purification process. Due to concentration limitations on smaller syntheses, only ^{1}H-NMR is used to characterize the molecule. ^{13}C-NMR is performed when quantity allows.

5.2: Cytotoxicity of Arvanil

As can be seen in Figure 14, the cytotoxicity of Arvanil is much higher than that of AEA. At 25 μM Arvanil is able to kill 90% of cancer cells within 24 hours while AEA is only able to kill 80% of cells at 200 μM within 24 hours. It is currently theorized that Arvanil follows the same mechanism of action as AEA. However, the addition of the vanillylamine functional group may cause a tighter binding to the intracellular target site or additional resistance to the FAAH enzyme allowing for a higher potency than AEA.

5.3: Cytotoxicity of 15d-$\Delta^{12,14}$-PMJ_2-Arvanil

In Figure 15 at 7.5 μM 15d-$\Delta^{12,14}$-PMJ_2 is able to kill 80% of cancer cells within 48 hours. However, 15d-$\Delta^{12,14}$-PMJ_2-Arvanil is incapable of killing more than 25% of cancer cells within 48 hours at the highest concentration tested (10 μM) and displays little to no cytotoxicity below this concentration. It is theorized that the bulky nature of the vanillylamine functional group prevents entry to the cell.

5.4: Formation of Micelles and Initial Characterization

Micelle formation was confirmed by fluorescence and the CMC determined as seen in Figure 18. Stability studies were also performed, as shown in Section 4.2 and Figure 19, and determined that micelles maintain a high level of stability at ambient temperature and atmosphere for up to two weeks due to the thermodynamic equilibrium present above the CMC. Currently the kinetic stability, present below the CMC, has not been characterized. The cytotoxic effect of the micelles was also determined as seen in Figure 22. A slight decrease in viability at 5.6 mg/mL but collectively no statistical effect can be noted. As the highest concentration to be

reached during loaded drug trials is 2.6 mg/mL, there is no direct effect expected from the micelles on cell viability.

5.5: Effect of Micelles on Drug Cytotoxicity

Initial studies have been performed with loaded micelles containing Arvanil. At this point, the micelles seem to be inhibiting the drug's cytotoxic abilities. It is currently theorized that the micelles are too stable in an in-vitro environment and are not able to disassemble to release the drug from the core of the micelle in a concentration capable of killing the cells.

5.6: Conclusions

The success of the anandamide, Arvanil, is a promising advancement for the second generation of the current treatment. This success indicates that other amide functional groups are capable of being added on to the molecule at the carboxylic acid and metabolized into the J-series prostaglandin equivalent. However, the failure of the metabolite, 15d-$\Delta^{12,14}$-PMJ_2-Arvanil, to produce any results similar to the AEA and 15d-$\Delta^{12,14}$-PMJ_2 relation may indicate the final or intermediate targets may be more specific than expected and could require additional study to better target with future molecules. Additionally, this may indicate that 15d-$\Delta^{12,14}$-PMJ_2-Arvanil is not capable of entering the cell at a noticeable rate to have an effect on cell viability.

The micelle drug delivery project is designed to create a delivery method for the hydrophobic therapeutics in the aqueous biologic environment of the human body. The micelles may also provide a solution for molecules that have difficulty entering the cell such as 15d-$\Delta^{12,14}$-PMJ_2-Arvanil due to their ability to endocytose into cells, thereby bypassing any transports or difficulty the drug molecule itself may face entering the cell. However, the current

formulation of micelles seems to be too stable in an in-vitro setting to successfully treat cells. A series of studies are planned to adjust the delivery protocol of the micelles to reach the ideal release of therapeutic molecules.

Overall, both the second-generation therapeutic project and the micelle delivery project have seen success. With confirmation that Arvanil can be synthesized and delivered to produce a more potent cytotoxic effect when compared to the arachidonic ethanolamide the second-generation project can be determined a success. The micelle delivery project has produced a successful protocol for production of loaded and unloaded micelles as well as developed methods for characterization of the micelles. The combination of these two successes may provide a path for future prostamide therapeutics and improvement of currently developed prostamides as well.

Future Directions

Adjustment of Micelle Protocols for In-vitro Delivery

As stated in Section 4.5, the DSPE: TPGS micelles seem to inhibit the cytotoxicity of Arvanil. A series of studies are underway to adjust the in-vitro delivery protocol with intent to match or exceed the cytotoxicity of Arvanil on its own. Initial studies involve adjusting the amount of FBS present in the treatment media to extend the treatment period of the cells as well as potentially destabilize the micelles. (Appendix C) Future adjustments include a reduction in micelle concentration similar to the dilution that will be experienced when injected in-vivo as well as adjusting the ratio of DSPE: TPGS and micelle: drug ratio.

Characterization of Loaded and Unloaded Micelles

Currently, a small amount of imaging has been completed on unloaded micelles using SEM. Future studies of empty micelles will involve lower concentrations as well as a higher magnification. Additionally, imaging of the loaded micelles containing both anandamides (AEA, Arv) and prostamides (15d-$\Delta^{12,14}$-PMJ_2, 15d-$\Delta^{12,14}$-PMJ_2-Arvanil). An understanding of both size and shape characteristics will allow for better application of the micelles as well as adjustment of formulation to better deliver therapeutics.

Determination of cytotoxicity of in-vivo loaded micelles

After determining the ideal formulation of micelles and delivery in-vitro. The loaded micelles will be delivered intravenously as opposed to intralesional injections that has been tested previously. The new form of injection will allow the micelles to be delivered systemically and is theorized to aggregate preferentially in tumors thus allowing the selective delivery of

therapeutic molecules to tumor sites. Further adjustment of formulation may be required to increase stability in a biologic environment.

Determination of the Final Destination of 15d-$\Delta^{12,14}$-PMJ_2-Arvanil

Depending on the success of 15d-$\Delta^{12,14}$-PMJ_2-Arvanil delivery in micelles, studies may be completed to determine where 15d-$\Delta^{12,14}$-PMJ_2-Arvanil interacts within the cell both to enter the cell as well as the intracellular targets that induce cell death. These methods may include fluorescent tagging of the 15d-$\Delta^{12,14}$-PMJ_2-Arvanil molecule or LC-MS to determine where in the cell the therapeutic is being sequestered.

References

(1) U.S. Cancer Statistics Working Group. *Cancer Statistics At a Glance*. U.S. Department of Health and Human Services. https://gis.cdc.gov/Cancer/USCS/#/AtAGlance/ (accessed 2023-04-02).

(2) Ladin, D. A.; Soliman, E.; Escobedo, R.; Fitzgerald, T. L.; Yang, L. V.; Burns, C.; Van Dross, R. Synthesis and Evaluation of the Novel Prostamide, 15-Deoxy, Δ12,14-Prostamide J2, as a Selective Antitumor Therapeutic. *Mol Cancer Ther* **2017**, *16* (5), 838–849. https://doi.org/10.1158/1535-7163.MCT-16-0484.

(3) National Cancer Institute. *What is Cancer?*. National Cancer Institute. https://www.cancer.gov/about-cancer/understanding/what-is-cancer (accessed 2023-04-02).

(4) National Cancer Institute. *What is Colorectal Cancer?*. National Cancer Institute. https://www.cancer.org/cancer/colon-rectal-cancer/about/what-is-colorectal-cancer.html (accessed 2023-04-02).

(5) American Cancer Society. *The Science Behind Radiation Therapy*. American Cancer Society. https://www.cancer.org/content/dam/CRC/PDF/Public/6151.00.pdf (accessed 2023-04-02).

(6) Ricciotti, E.; FitzGerald, G. A. Prostaglandins and Inflammation. *Arterioscler Thromb Vasc Biol* **2011**, *31* (5), 986–1000. https://doi.org/10.1161/ATVBAHA.110.207449.

(7) Jowsey, I. R.; Thomson, A. M.; Flanagan, J. U.; Murdock, P. R.; Moore, G. B.; Meyer, D. J.; Murphy, G. J.; Smith, S. A.; Hayes, J. D. Mammalian Class Sigma Glutathione S-

Transferases: Catalytic Properties and Tissue-Specific Expression of Human and Rat GSH-Dependent Prostaglandin D2 Synthases. *Biochem J* **2001**, *359* (Pt 3), 507–516. https://doi.org/10.1042/0264-6021:3590507.

(8) Shibata, T.; Kondo, M.; Osawa, T.; Shibata, N.; Kobayashi, M.; Uchida, K. 15-Deoxy-Δ12,14-Prostaglandin J2. *Journal of Biological Chemistry* **2002**, *277* (12), 10459–10466. https://doi.org/10.1074/jbc.M110314200.

(9) Narumiya, S.; FitzGerald, G. A. Genetic and Pharmacological Analysis of Prostanoid Receptor Function. *Journal of Clinical Investigation* **2001**, *108* (1), 25–30. https://doi.org/10.1172/JCI13455.

(10) Soliman, E.; Van Dross, R. Anandamide-Induced Endoplasmic Reticulum Stress and Apoptosis Are Mediated by Oxidative Stress in Non-Melanoma Skin Cancer: Receptor-Independent Endocannabinoid Signaling. *Mol Carcinog* **2016**, *55* (11), 1807–1821. https://doi.org/10.1002/mc.22429.

(11) Ladin, D. A.; Nelson, M. M.; Cota, E.; Colonna, C.; Burns, C.; Robidoux, J.; Fisher-Wellman, K. H.; Van Dross-Anderson, R. Calcium Signaling Induced by 15-Deoxy-Prostamide-J2 Promotes Cell Death by Activating PERK, IP3R, and the Mitochondrial Permeability Transition Pore. *Oncotarget* **2022**, *13*, 1380–1396. https://doi.org/10.18632/oncotarget.28334.

(12) Morris, A. Developing Novel Chemotherapeutics: A Structure-Activity Study of Anandamide Analogs and Their Cytotoxic Profiles. Dissertation, East Carolina University, Greenville, 2019.

(13) Prusakiewicz, J. J.; Turman, M. V.; Vila, A.; Ball, H. L.; Al-Mestarihi, A. H.; Marzo, V. Di; Marnett, L. J. Oxidative Metabolism of Lipoamino Acids and Vanilloids by Lipoxygenases and Cyclooxygenases. *Arch Biochem Biophys* **2007**, *464* (2), 260–268. https://doi.org/10.1016/j.abb.2007.04.007.

(14) Dabholkar, R. D.; Sawant, R. M.; Mongayt, D. A.; Devarajan, P. V.; Torchilin, V. P. Polyethylene Glycol–Phosphatidylethanolamine Conjugate (PEG–PE)-Based Mixed Micelles: Some Properties, Loading with Paclitaxel, and Modulation of P-Glycoprotein-Mediated Efflux. *Int J Pharm* **2006**, *315* (1–2), 148–157. https://doi.org/10.1016/j.ijpharm.2006.02.018.

(15) Zhang, J.; Shen, L.; Li, X.; Song, W.; Liu, Y.; Huang, L. Nanoformulated Codelivery of Quercetin and Alantolactone Promotes an Antitumor Response through Synergistic Immunogenic Cell Death for Microsatellite-Stable Colorectal Cancer. *ACS Nano* **2019**, *13* (11), 12511–12524. https://doi.org/10.1021/acsnano.9b02875.

(16) Hou, L.; Fan, Y.; Yao, J.; Zhou, J.; Li, C.; Fang, Z.; Zhang, Q. Low Molecular Weight Heparin-All-Trans-Retinoid Acid Conjugate as a Drug Carrier for Combination Cancer Chemotherapy of Paclitaxel and All-Trans-Retinoid Acid. *Carbohydr Polym* **2011**, *86* (3), 1157–1166. https://doi.org/10.1016/j.carbpol.2011.06.008.

(17) Ghezzi, M.; Pescina, S.; Padula, C.; Santi, P.; Del Favero, E.; Cantù, L.; Nicoli, S. Polymeric Micelles in Drug Delivery: An Insight of the Techniques for Their Characterization and Assessment in Biorelevant Conditions. *Journal of Controlled Release* **2021**, *332*, 312–336. https://doi.org/10.1016/j.jconrel.2021.02.031.

(18) Gu, P.; Xu; Sui; Gou; Meng; Sun; Wang; Qi; Zhang; He; Tang. Polymeric Micelles Based on Poly(Ethylene Glycol) Block Poly(Racemic Amino Acids) Hybrid Polypeptides: Conformation-Facilitated Drug-Loading Behavior and Potential Application as Effective Anticancer Drug Carriers. *Int J Nanomedicine* **2012**, 109. https://doi.org/10.2147/IJN.S27475.

Appendix A: IACUC Approval Letter

August 4, 2022

North Carolina Biotechnology Center - NCBC

Dear Sir or Madam:

The vertebrate animal use in the following application submitted to the NCBC was reviewed and is congruent with an IACUC-approved animal use protocol.

Title of Application: *Targeting Multiple Cancer Types by Micellar Delivery of the Immunotherapeutic 15-deoxy-D12,14-Prostamide J2.*

Name of the Principal Investigator: Van Dross, Rukiyah, Ph.D.

Name of Institution: East Carolina University

Congruency approval: August 3, 2022

Animal Use Protocol Expiration Date: W252a – June 5, 2023

This institution is fully accredited by AAALAC and has animal Welfare Assurance on file with the Office of Laboratory Animal Welfare. The Assurance number is D16-00294.

Sincerely yours,

Susan McRae, Ph.D.
Chair, Animal Care and Use committee

SM/GD

cc: ECU Office of Research Administration

Appendix B. Characterization of Therapeutic Molecules

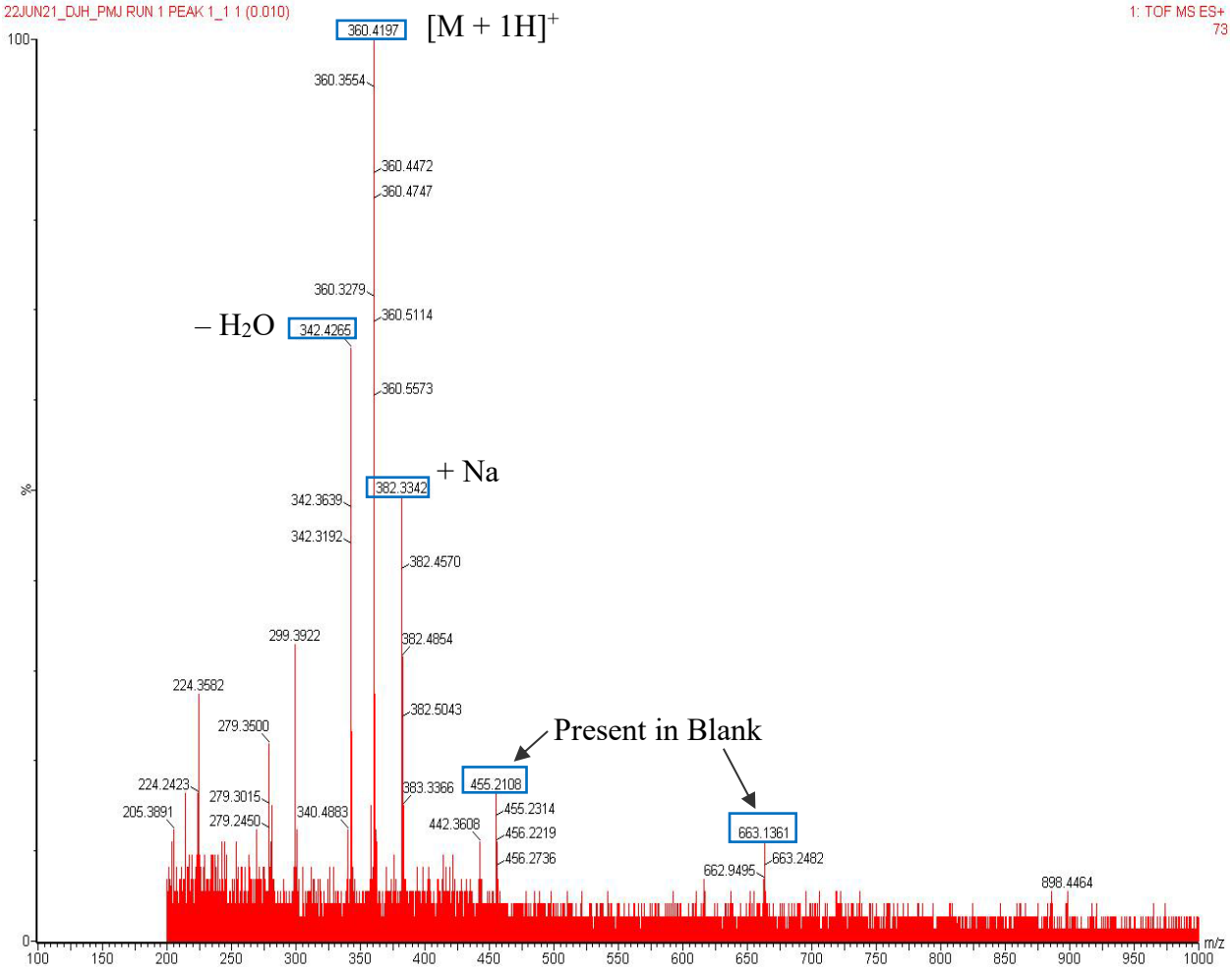

Figure 23. Time of Flight Positive Ion ESI-MS of 15d-$\Delta^{12,14}$-PMJ$_2$

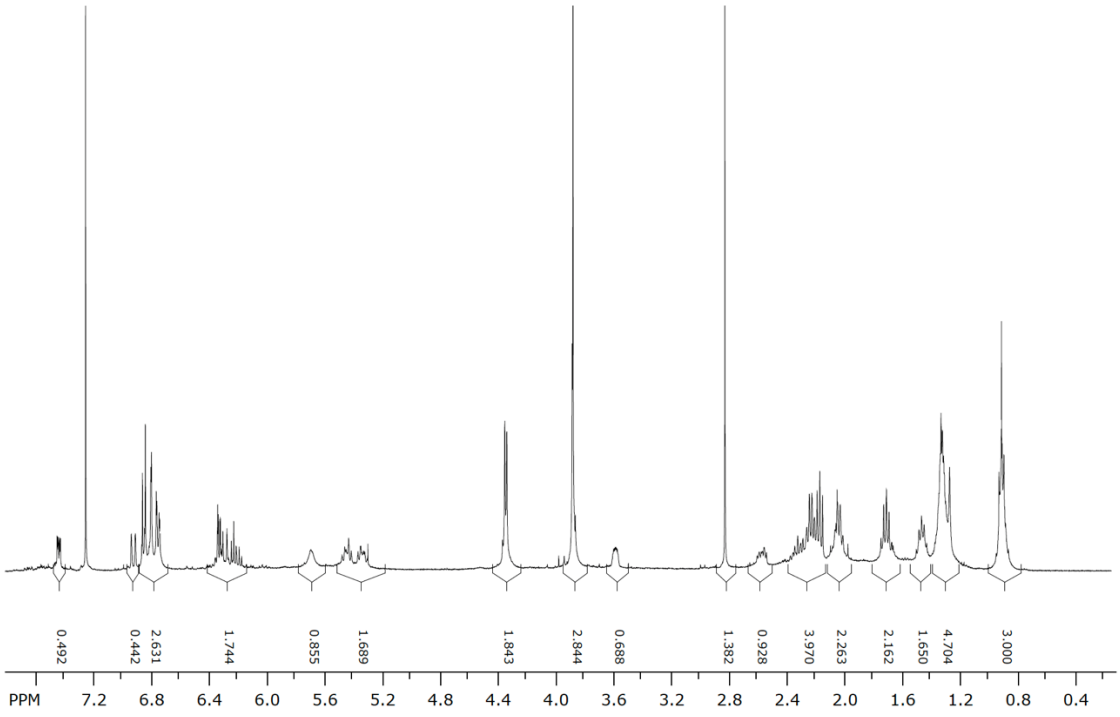

Figure 24. Integrated Proton NMR of Arvanil

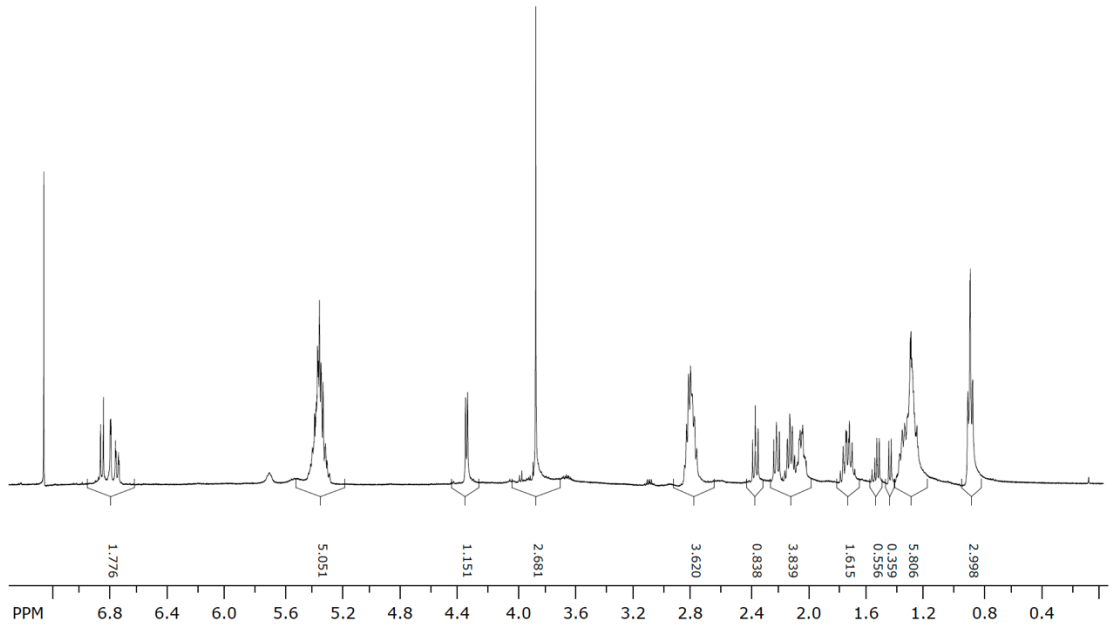

Figure 25. Integrated Proton NMR of 15d-$\Delta^{12,14}$-PMJ$_2$-Arvanil

Appendix C. In-Vitro Micelle Studies

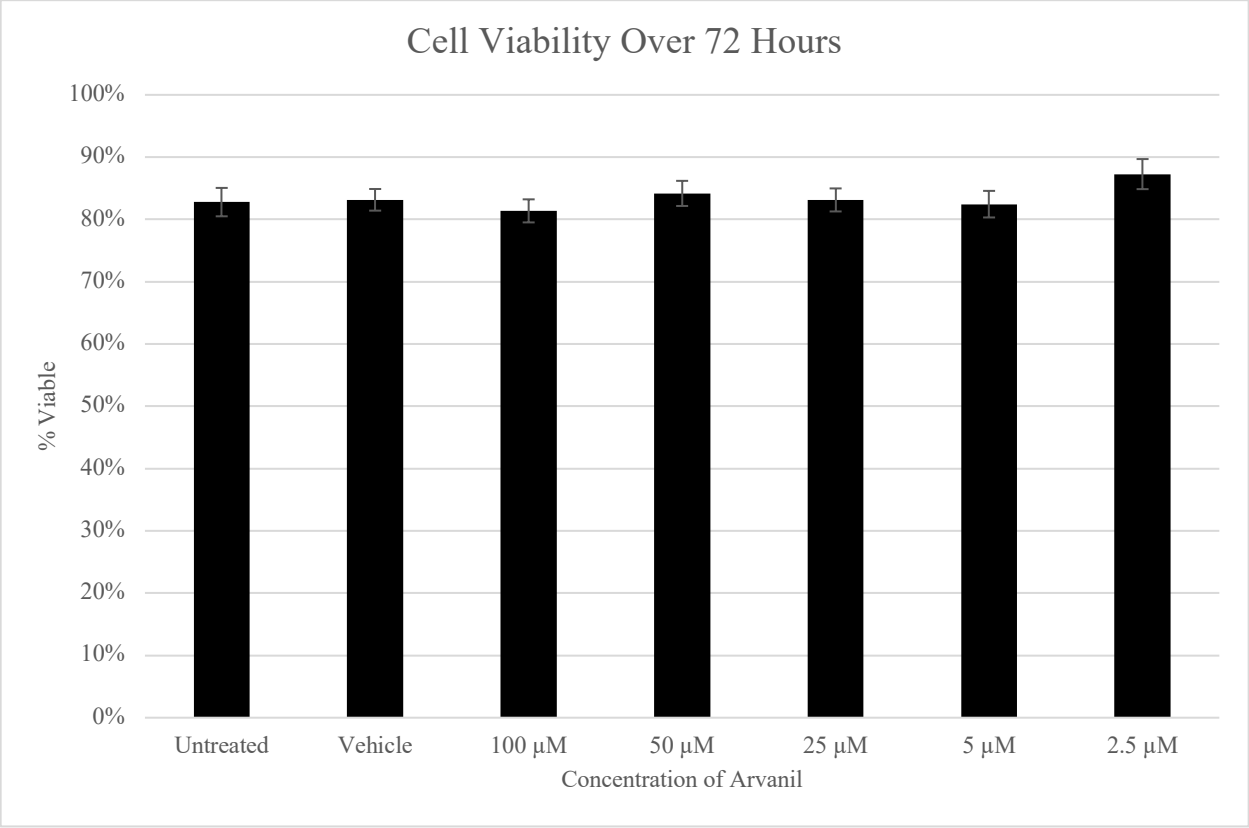

Figure 26. Cell Viability of Arvanil Loaded Micelles in a 1% FBS DMEM Media with HCA-7 Cells